

VLA Scientific Memo. No. 173

## Application of Fast Switching Phase Calibration at mm Wavelengths on 33 km Baselines<sup>1</sup>

**C.L. Carilli and M.A. Holdaway**

National Radio Astronomy Observatory

Socorro, NM, 87801

May 22, 1997

### Abstract

We present a series of tests of the Fast Switching (FS) phase calibration technique using the Very Large Array (VLA) at mm wavelengths on baselines out to 33 km. These tests demonstrate that FS phase calibration with cycle times  $\approx 100$  sec can result in diffraction limited images of faint sources at 7mm in the largest configurations of the VLA under good weather conditions. There are times however when shorter cycle times may be required. We present examples using both ‘control sources’ (ie. celestial calibrators), and a faint source of astronomical interest: the M2 supergiant star Betelgeuse ( $\alpha$  Orionis). A diffraction limited resolution image (40 mas resolution) of the surface of Betelgeuse was obtained showing a resolved radio photosphere with mean  $T_B = 3500$  K and diameter = 80 mas, consistent with theoretical models of this star.

We also present the tropospheric root phase structure function on baselines ranging

---

<sup>1</sup>This memo is based on a presentation given at the Japan-US workshop on ‘Millimeter and Submillimeter Astronomy at 10 mas Resolution,’ March 1997, Nobeyama Radio Observatory Report No. 430, eds. M. Ishiguro and R. Kawabe, p. 39

from 200m to 20000m. This function shows the three regimes predicted by Kolmogorov turbulence theory: On short baselines ( $b \leq 1.2$  km) the measured power-law index is  $n = 0.85 \pm 0.03$ , while the predicted value is 0.83 (thick screen). On intermediate baselines ( $1.2 \leq b \leq 6$  km) the measured index is  $0.41 \pm 0.03$  and the predicted value is 0.33 (thin screen). On long baselines ( $b \geq 6$  km) the measured index is  $0.1 \pm 0.2$  and the predicted value is zero (outer scale). The implication is that the vertical extent of the turbulent boundary layer is about 1 km, and that the outer scale of the turbulence is 6 km, although the long baseline data suggests that the outer scale may be anisotropic.

## 1. Introduction

In the fourth quarter of 1996 (October 1996 to January 1997) the Very Large Array was in its 33km configuration (‘A array’). During this period antennas with 7 mm receivers were situated at the ends of each arm in order to obtain the full resolution of the array for the first time (40 mas). The theoretical sensitivity for the array is 0.1 mJy in 12hrs at 7 mm (13 antennas, 50 MHz bandwidth, 2polarizations, 2IFs), hence the brightness temperature sensitivity is 60 K at 40 mas resolution. These baselines are an order of magnitude longer than for any previous connected-element interferometer operating at mm wavelengths.

One reason for going to the longest baselines with the 7 mm antennas at the VLA was to test whether the Fast Switching (FS) phase calibration technique would allow for diffraction limited imaging of faint sources on the longest baselines (Carilli, Holdaway, and Sowinski 1996, Holdaway and Owen 1995). Otherwise, the spatial resolution will be limited by tropospheric ‘seeing’:

$$\Theta_s \approx \frac{\lambda}{r_o} \text{ rad},$$

where  $\lambda$  = observing wavelength, and  $r_o$  = the transverse scale over which the rms phase difference equals one radian (Narayan et al. 1990). Even under the best conditions at the VLA the limiting resolution would be about 0.4'' due to tropospheric phase fluctuations. Fast Switching phase calibration entails standard phase transfer from a strong celestial calibration source to a faint target source using a cycle time short enough to ‘stop’ the tropospheric phase fluctuations at level well below 1 rad. We will show that under typical conditions at the VLA during the fourth quarter of 1996, the FS technique was adequate to obtain images of faint sources with *diffraction limited* spatial resolution on *arbitrarily long* baselines at 7 mm.

## 2. The Root Phase Structure Function in BnA array

Phase variations due to the troposphere are caused by temporal changes in the water vapor content. The implied changes in index of refraction are non-dispersive, and hence the phase-variations will increase linearly with frequency (Tatarskii 1978). The standard model for these fluctuations is the ‘frozen screen’ approximation, in which variations in the water vapor column density occur in a turbulent layer in the troposphere at some height,  $H$ , with some vertical extent,  $W$ , which convects across the array at some velocity,  $V_A$ . The convection timescale for water vapor irregularities is assumed to be shorter than the dissipation (or diffusion) timescale and hence the phase screen is ‘frozen-in’ to the flow (Taylor 1938, Wright 1996). Under this assumption one can relate temporal and spatial phase fluctuations using  $V_A$ .

Tropospheric phase fluctuations are usually characterized by a root phase structure function,  $\Phi_{rms}(b)$ , equal to the root mean square phase variations on baselines of length  $b$ , when calculated over a sufficiently long time (time  $\gg$  baseline crossing time =  $\frac{b}{V_A}$ ), or for an ensemble of measurements at a given time on many baselines of length  $b$ . Kolmogorov turbulence theory (Coulman 1990) predicts a function of the form:

$$\Phi_{rms}(b) = \frac{K}{\lambda} b^n \quad \text{degrees}$$

where  $b$  is in km, and  $\lambda$  is in cm. Typical values of  $K$  for the VLA can be found in Carilli et al. (1996).

Kolmogorov turbulence theory predicts  $n = \frac{1}{3}$  for baselines longer than  $W$ , and  $n = \frac{5}{6}$  for baselines shorter than  $W$  (Coulman 1990). The change in power-law index at  $b = W$  is due to the finite vertical extent of the turbulent boundary layer. For baselines shorter than the typical turbulent layer extent the full 3-dimensionality of the turbulence is involved (thick-screen), while for longer baselines a 2-dimensional approximation applies

(thin-screen). Turbulence theory also predicts an ‘outer-scale’,  $L_o$ , beyond which the structure function should be flat ( $n = 0$ ). This scale corresponds to the largest coherent structures, or maximum correlation length, for water vapor fluctuations in the troposphere, presumably set by external boundary conditions.

Measurements of the root phase structure function have been made on baselines out to 3 km (Sramek 1990, Holdaway et al. 1995, Holdaway and Owen 1995, Wright 1996, Carilli et al. 1996). These measurements have demonstrated the basic broken power-law behavior ( $n = 5/6$  to  $n = 1/3$ ), with the transition occurring at about 1 km, although power-laws of intermediate indices have also been seen (Holdaway and Owen 1995, Holdaway et al. 1995). However, to date no measurement has been made of the full structure function, from  $b \ll W$  to  $b \gg L_o$ . The difficulty is that the outer scale is predicted to be of order 10 km (Coulman 1990), thereby requiring the A configuration of the VLA. However, the shortest baselines in the A configuration are about 1 km, hence observations with the A array alone do not sample  $b < W$ .

As part of our testing with the VLA we performed a measurement of the root phase structure function using the mixed BnA configuration. This configuration has good baseline coverage ranging from 200m to 20 km, hence sampling all three ranges in the structure function. The resulting root phase structure function is shown in Figure 1, for 13 mm observations made during the night of Jan. 27, 1997 on the VLA calibration source 0748+240. The total observing time was 90 min, corresponding to a tropospheric travel distance of 54 km, assuming  $V_A = 10 \text{ m s}^{-1}$  (see below). Below we shall find that 54 km is much larger than the outer scale of the turbulence, hence 90 minutes corresponds to many realizations of the phase screen at  $b = L_o$ .

The open circles show the nominal tropospheric root phase structure function = rms phases for the visibilities versus baseline length calculated over the full 90 min time

range. The solid squares are the rms phases after subtracting (in quadrature) a constant electronic noise term of  $10^\circ$ , as derived from the data by requiring the best power-law on short baselines. The  $10^\circ$  noise term is consistent with previous measurements at the VLA indicating electronic phase noise increasing with frequency as  $0.5^\circ$  per GHz (Carilli and Holdaway 1996).

The three regimes of the structure function as predicted by theory are verified very nicely in Figure 1, and the observed power-law indices are in good agreement with the predicted values. On short baselines ( $b \leq W = 1.2$  km) the measured index  $n = 0.85 \pm 0.03$ , while the predicted value is 0.83. On intermediate baselines ( $W \leq b \leq L_o = 6$  km) the measured index is  $0.41 \pm 0.03$  and the predicted value is 0.33. On long baselines ( $b \geq L_o = 6$  km) the measured index is  $0.1 \pm 0.2$  and the predicted value is zero. The implication is that the vertical extent of the turbulent boundary layer is about 1 km, and that the outer scale of the turbulence is 6 km.<sup>2</sup>

Another trend that is clear in Figure 1 is that the scatter increases significantly beyond the outer scale. A possible explanation for this increased scatter is shown in Figure 2. The open circles in Figure 2 are rms phases for baselines between antennas on the north arm and the south-west arm of the array. The filled squares are rms phases for baselines between antennas on the north arm and the south-east arm of the array. The two functions are similar (to within the noise) out to about 6 km. Beyond 6 km the open circles continue to rise, while the filled squares flatten to zero slope. This trend may indicate an

---

<sup>2</sup>One potential problem with this outer scale analysis is that we are getting only a couple of tropospheric crossing times for the longest spacings of the array (33 km) during the 90 min observation. We plan longer observations in the next BnA array to verify that the outer scale measured for the current observations is not an artefact of limited statistics on the longest baselines.

anisotropic outer scale, such that the structure function ‘saturates’ at different baseline lengths depending on the orientation of the baseline. An anisotropic outer scale could arise e.g., due to anisotropic boundary conditions. For completeness we note that the ground wind speed during these observations was  $2 \text{ m s}^{-1}$  from the southeast, ie. parallel to the southeast arm. It is important to keep in mind that the ground wind speed may bear little relation to the more relevant speed of the winds aloft.

### 3. Fast Switching in BnA Array

As a demonstration of the effectiveness of fast switching phase calibration, we have calculated the root phase SF for the BnA array data at 13 mm after applying antenna-based phase solutions averaged over increasingly shorter timescales. The results are shown in Figure 2. The solid squares show the nominal tropospheric root phase SF from Figure 1, but now on a linear scale. The open circles are the rms phases of the visibilities after applying antenna based phase solutions averaged over 300 sec. The stars are the rms phases of the visibilities after applying antenna based phase solutions averaged over 20 sec.

The residual root SF using a 300 sec calibration cycle parallels the nominal tropospheric root SF out to a baseline length of 1500m, beyond which the root SF saturates at a constant rms phase value of  $20^\circ$ . Calibrating with relatively short cycle times ‘stops’ the tropospheric phase variations at an effective baseline length:  $b_{eff} = \frac{V_A \times t_{ave}}{2}$  (Carilli et al. 1996). The implied wind velocity is then:  $V_A = \frac{2 \times 1500m}{300sec} = 10 \text{ m s}^{-1}$ . Going to a 20 sec calibration cycle reduces  $b_{eff}$  to only 100 m, which is shorter than the shortest baseline of the array, and the saturation rms is  $5^\circ$ .

The important point is that, after applying standard phase calibration techniques on timescales short compared to the tropospheric crossing, the resulting rms phase fluctuations

are independent of baseline length for  $b > b_{eff}$ .

#### 4. Applying FS Phase Calibration at 7 mm on 33 km Baselines

Fast Switching phase calibration was employed extensively at 7 mm during the fourth quarter of 1997. We present one example in which FS calibration was effective in allowing for diffraction limited imaging of a faint celestial target source. The target source was the M2 supergiant star Betelgeuse ( $\alpha$  Orionis). The optical photospheric diameter for the star is 65 mas (Tuthill et al. 1997), while the integrated flux density of the star is 27 mJy at 7 mm. Hence the star is large enough to be resolved by the VLA at 40 mas resolution, and bright enough to be detected, but not bright enough to allow for self-calibration on short timescales. Diffraction limited imaging of the star requires the FS phase transfer technique.

The Betelgeuse observations were made over the night of December 21, 1996. We used the celestial calibrator 0552+032 located  $4^\circ$  degrees from the target source, with a total cycle time of 150 sec. Figure 4 shows the time series of antenna-based phase solutions on the calibrator for these observations for three antennas on the north arm of the VLA. The total observing time was 10hrs. The phase stability was excellent between IAT 3:00 and 9:00. After 9:00 the phase stability deteriorated significantly. Figure 5 shows images of Betelgeuse made by applying the FS phase calibration solutions from 0552+032. Figure 5A shows the image made from data taken during the time when the phase stability was good (3 - 9 IAT), while Figure 5B shows the image made from data taken during the time when the phase stability deteriorated (9 - 12 IAT). The image from the good time period reveals a resolved, possibly asymmetric source, with a diameter of about 80 mas and an average brightness temperature of 3500 K, as expected for the radio photosphere of this M2 supergiant (Lim et al. 1997). The image from the bad time range reveals a source, but the structure and brightness are uncertain due to the poor phase stability. In other words, the



150 sec cycle was adequate to obtain reasonable phase transfer from the calibrator to the source during good weather, but was inadequate when the weather deteriorated. It is likely that a faster cycle time might have been able to recover a reasonable image of the source even during the bad time period. The observing log reports an increase in the ground wind speed from  $2.9 \text{ m s}^{-1}$  to  $5.5 \text{ m s}^{-1}$ , and an increase in stratusform-type cloud cover from 50% to 100%, during the time period when the phase stability deteriorated.

In Figure 6 we show the root phase structure functions for the periods of good and bad weather for the December 21 observations. Also shown are the residual root SFs after self-calibration with a 35 sec averaging time. Two trends are apparent. The first is that during the bad time period the steep part of the structure function continues to longer baselines ( $> 10 \text{ km}$ ). The second is that the residual saturation RMS (after self-calibration) increases from  $8^\circ$  during the good time period to  $14^\circ$  during the bad time period. The possible implications are that: (i) the turbulent region in the troposphere became thicker during the bad time period, and (ii) the amplitude in the structure function (the ‘K’ value) increased, from about 24 during the good time period, to 42 during the bad time period.

As an independent check on possible extraneous structure introduced by residual tropospheric phase variations after FS phase calibration, we used two 15min time periods during the December observations to switch between the calibrator 0552+032 and a ‘control source,’ namely the celestial calibrator 0532+075, with the same cycle time as was employed on Betelgeuse. The results are shown in Figure 7. Figure 7A shows the image of the control source 0532+075 made after self-calibration with an averaging time of 10sec (the nominal ‘true’ image). Figure 7B shows the image of 0532+075 made by transferring phase solutions from the 0552+032 with an averaging time of 900 sec. Figure 7C shows the image of 0532+075 made by transferring phase solutions from the 0552+032 with a cycle time of 150sec. The 900 sec cycle time results in an extended image, while the 150 sec cycle time

shows a point source with some minor structure due to residual phase errors. The image coherence increases from 42% with a 900 sec calibration cycle time to 72% with a 150 sec cycle time, where the coherence is defined as the ratio of the peak surface brightness on the phase-referenced image relative to that seen on the self-calibrated image.

## 5. Conclusions

We have demonstrated that the FS phase calibration technique with cycle times  $\approx 100$  sec can result in diffraction limited images of faint sources in the largest configurations of the VLA under good weather conditions. There are times however when shorter cycle times may be required. The NRAO has installed at the VLA site a two element interferometer tracking a satellite beacon at 11.3 GHz to act as a monitor of the tropospheric phase stability (Radford et al. 1996). Data from this monitor should help observers in making real-time decisions concerning required calibration cycle times for high frequency observations with the VLA, as well as provide a quantitative seasonal and diurnal record of the phase stability of the VLA site, in order to facilitate efficient scheduling of observing programs that are sensitive to tropospheric phase fluctuations.

## References

- Carilli, C.L., Holdaway, M.A., and Sowinski, K. 1996, VLA Scientific Memo. No. 169
- Carilli, C.L. and Holdaway, M.A. 1996, VLA Scientific Memo. No. 171
- Coulman, C.E. 1990, in *Radio Astronomical Seeing*, eds. J. Baldwin and S. Wang, (Pergamon: New York), p. 11.
- Holdaway, M.A., Radford, S., Owen, F., and Foster, S. 1995, MMA Memo. Series.
- Holdaway, M.A. and Owen, F.N. 1995, MMA Memo. No. 126
- Holdaway, M.A. Owen, F., and Rupen, M.P. 1994, MMA Memo. No. 123
- Holdaway, M.A. 1992, MMA Memo. No. 84
- Lim, J., Carilli, C.L., White, S., Beasley, A., and Marson, R. 1997, in preparation
- Narayan, R., Anatharamiah, K., and Cornwell, T. 1990, in *Radio Astronomical Seeing*, eds. J. Baldwin and S. Wang, (Pergamon: New York), p. 205
- Radford, S.J., Reiland, G., and Shillue, B. 1996, P.A.S.P., 108, 441
- Sramek, R. 1990, in *Radio Astronomical Seeing*, eds. J. Baldwin and S. Wang, (Pergamon: New York), p. 21
- Tatarskii, V.I. 1961, *Wave Propagation in Turbulent Media*, (New York: Wiley)
- Taylor, G.I. 1938, Proc. R. Soc. London A, 164, 476
- Tuthill, P.G., Haiff, C.A., and Baldwin, J.E. 1997, M.N.R.A.S., 285, 529
- Wright, M.C.H. 1996, P.A.S.P., 108, 520

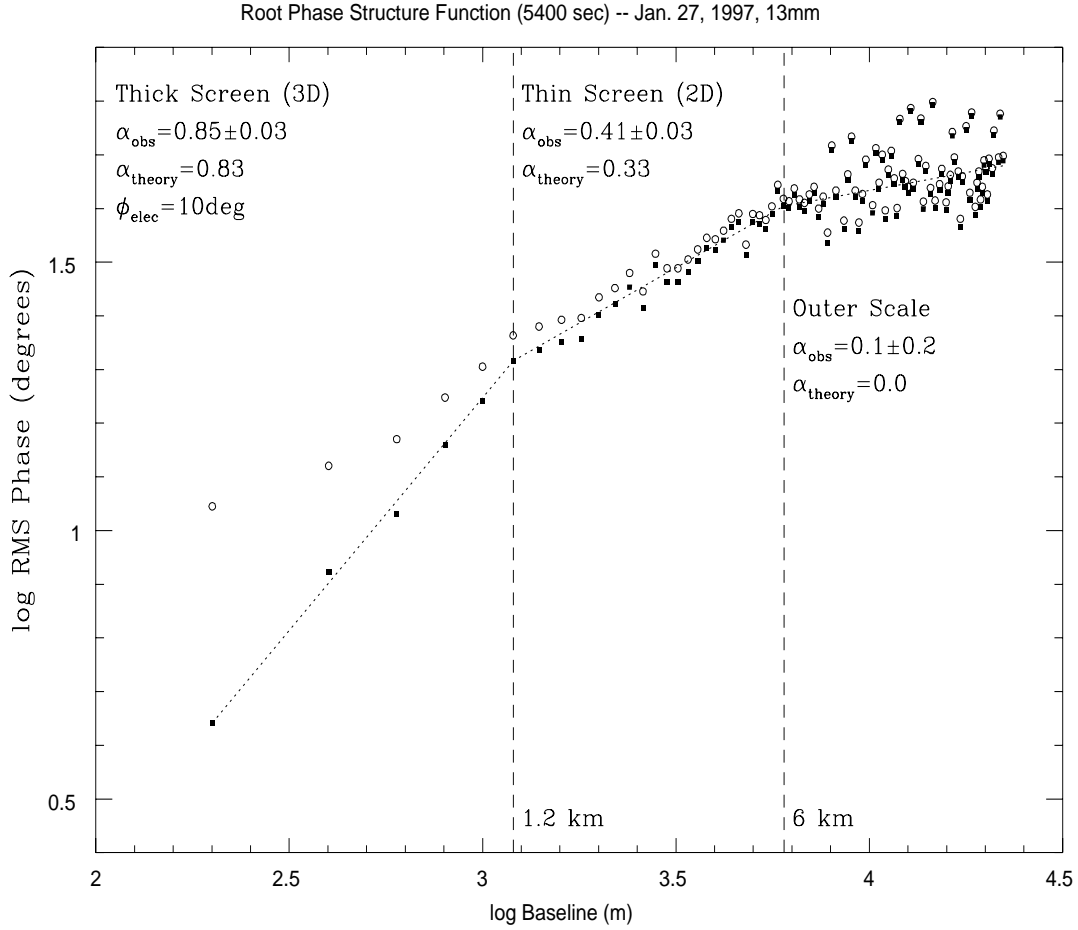


Fig. 1.— The root phase structure function from observations at 13 mm in the BnA array of the VLA on January 27, 1997. The open circles show the rms phase variations versus baseline length measured on the VLA calibrator 0748+240 over a period of 90 min. The filled squares show these same values with a constant noise term of  $10^\circ$  subtracted in quadrature.

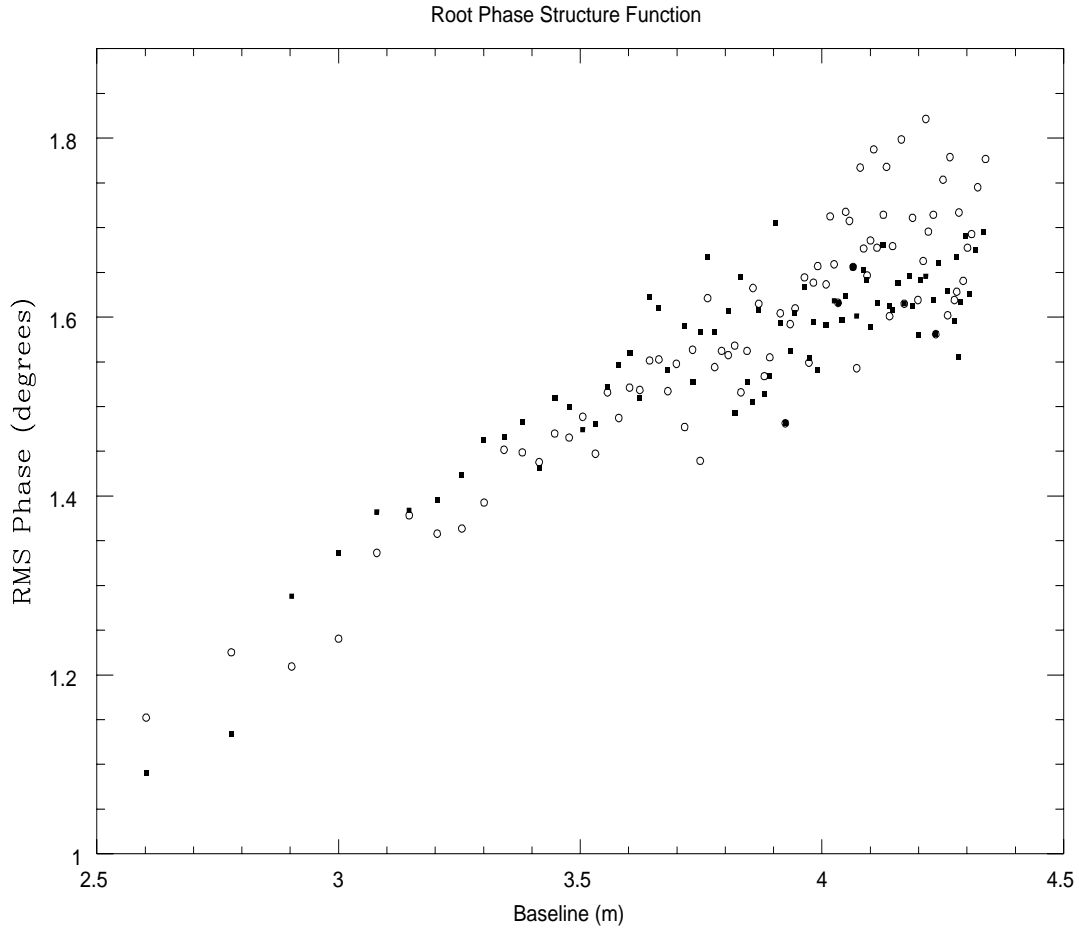


Fig. 2.— Same as Figure 1, but now the open circles are the root phase structure function for baselines between antennas on the north arm of the array with those on the southwest arm, while the filled squares are for baselines between antennas on the north arm with those on the southeast arm.

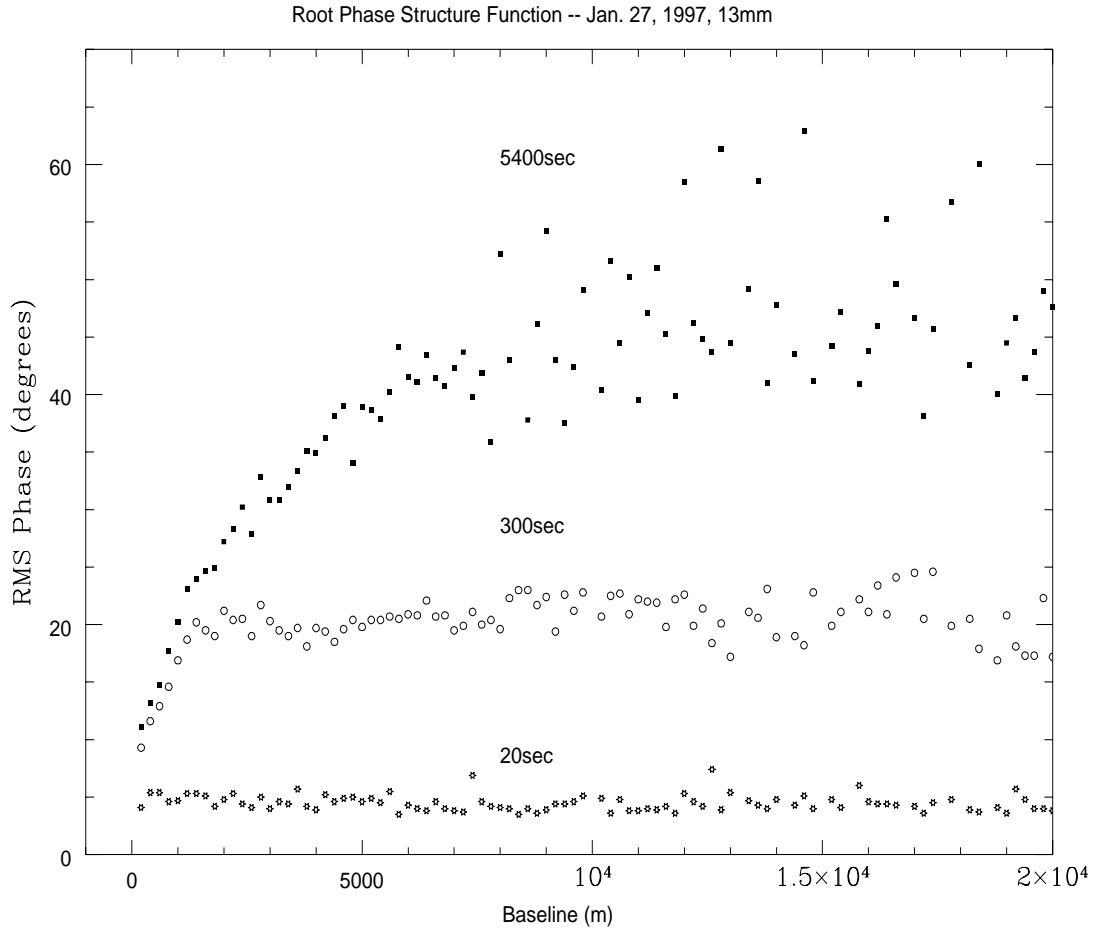


Fig. 3.— The solid squares are the same as for Figure 1, but now on a linear scale. The open circles show the residual rms phase variations versus baseline length after calibrating with a cycle time of 300sec. The open stars show the residual rms phase variations versus baseline length after calibrating with a cycle time of 20sec.

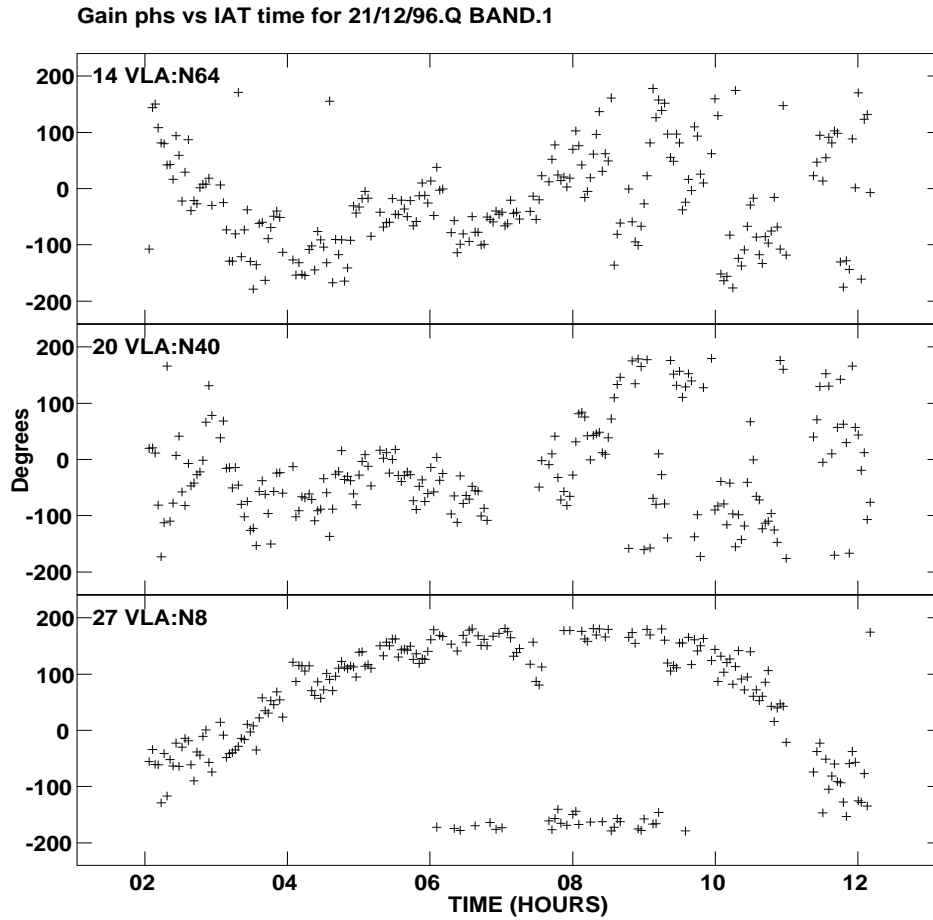


Fig. 4.— The time series of antenna-based phase solutions on the calibrator 0552+032 for three antennas on the north arm at 7 mm on December 21, 1996.

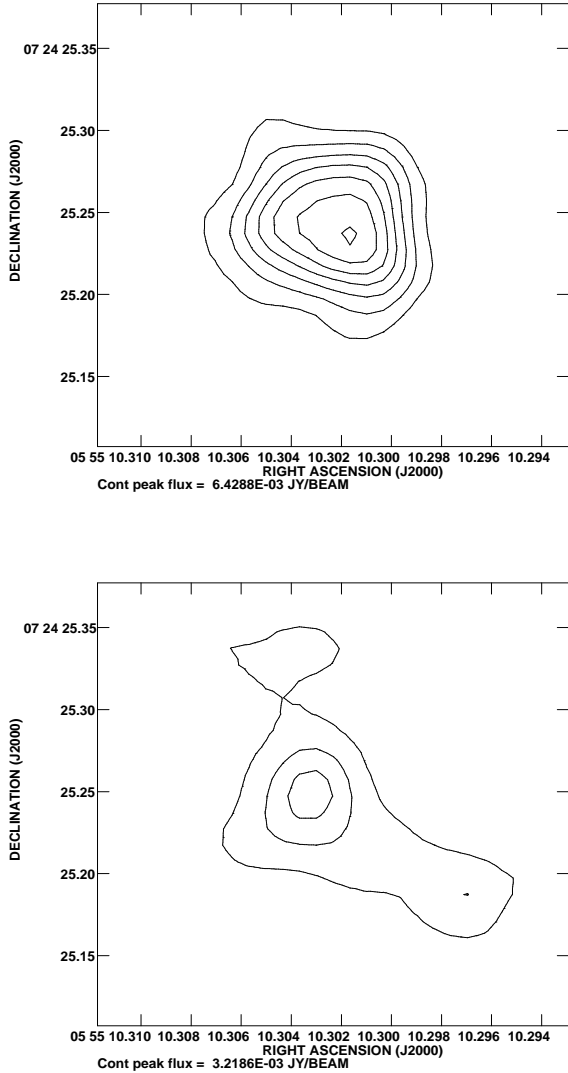


Fig. 5.— The top figure shows an image of the star Betelgeuse at 7 mm, 40mas resolution made from data taken during the time period of good phase stability (3 - 9 IAT) the night of Dec. 21, 1997. The lower image shows the image of Betelgeuse made from data taken during the time period of bad phase stability (9 - 12 IAT) IAT). The contour levels are -1.8, -0.9, 0.9, 1.8, 2.7, 3.6, 4.5, 5.4, and 6.3 mJy/beam.



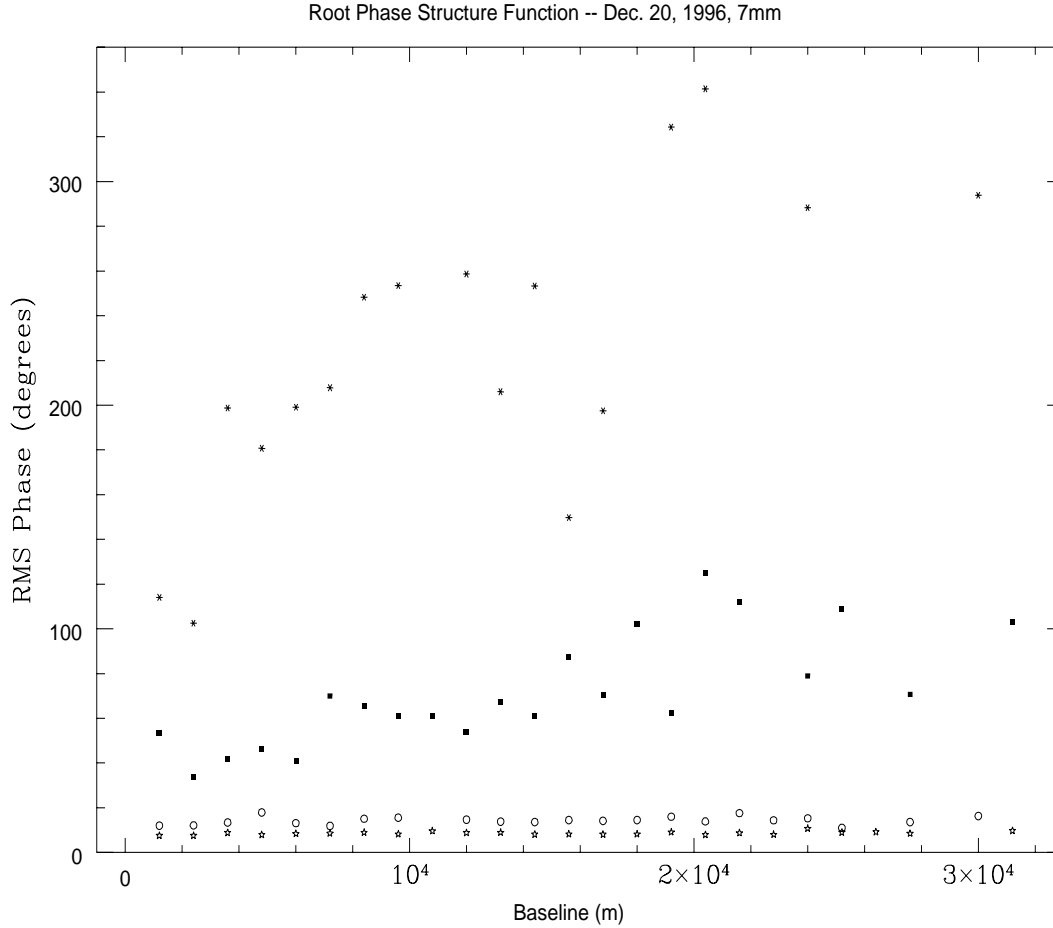


Fig. 6.— The rms phase variations versus baseline length measured on the calibrator 0552+032 on Dec. 21, 1997 at 7 mm with the VLA. The stars are the rms phases from the bad phase stability time period (9 - 12 IAT). The solid squares are the rms phases from the good time period (3 - 9 IAT). The open circles are the residual rms phases from the bad time period after applying phase calibration with a 35 sec averaging time. The open stars are the residual rms phases from the good time period after applying phase calibration with a 35 sec averaging time.

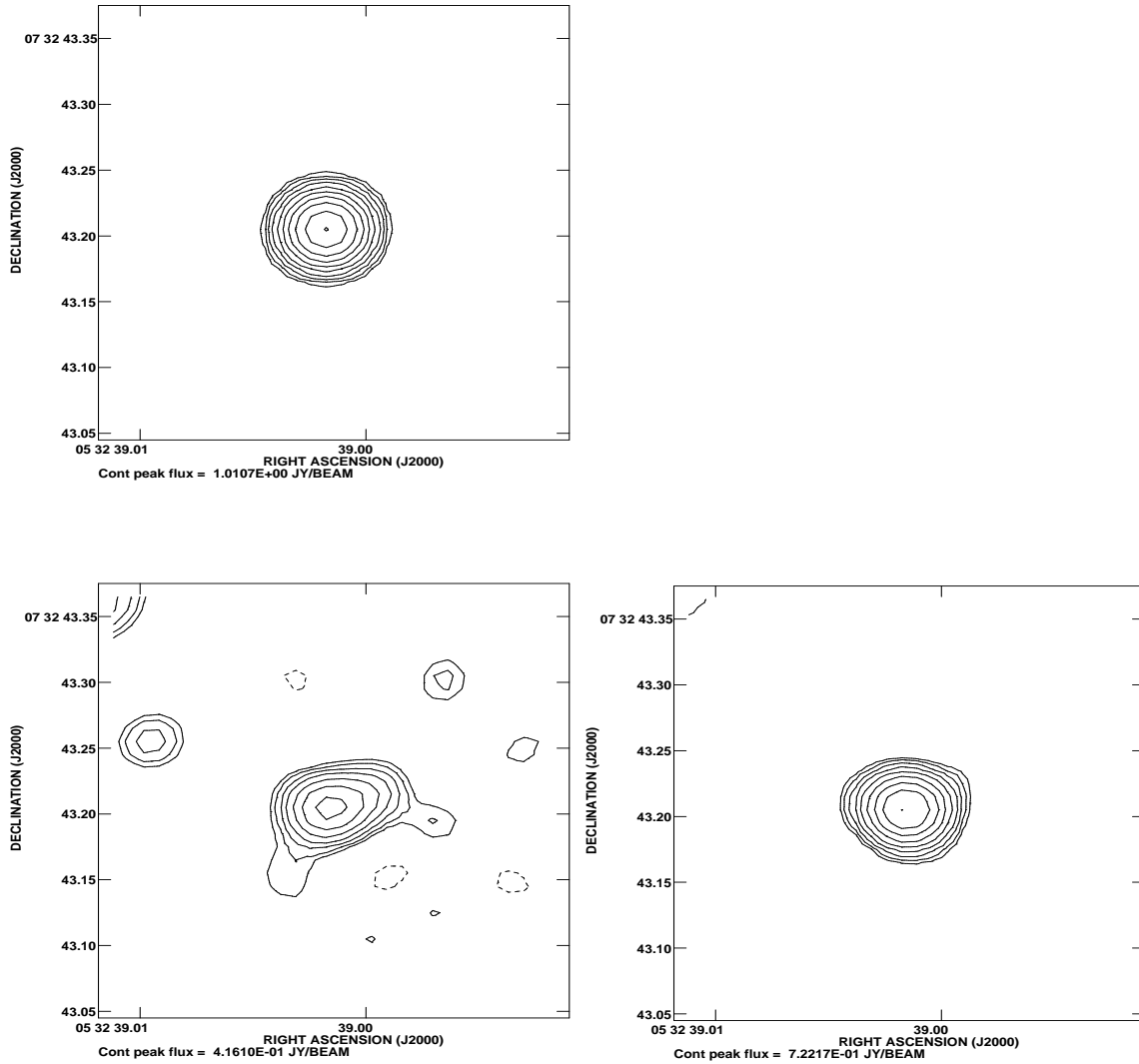


Fig. 7.— The top figure shows an image at 7 mm, 40 mas resolution of the control source, VLA calibrator 0532+075, after self-calibrating the phases with an averaging time of 10 sec. The bottom left figure shows an image of 0532+075 made after transferring phase solutions determined on 0552+032 averaged over 15 min. The bottom right figure shows an image of 0532+075, made after transferring phase solutions determined on 0552+032 with a cycle time of 150 sec. The contour levels are a geometric progression in the square root of two, with the first level being 45 mJy/beam. Dotted contours are negative.